Laser Spectroscopy of Niobium Fission Fragments: First Use of Optical Pumping in an Ion Beam Cooler Buncher

B. Cheal,[1,*] K. Baczynska,[2] J. Billowes,[1] P. Campbell,[1] F. C. Charlwood,[1] T. Eronen,[3] D. H. Forest,[2] A. Jokinen,[3] T. Kessler,[3] I. D. Moore,[3] M. Reponen,[3] S. Rothe,[4] M. Rüffer,[2] A. Saastamoinen,[3] G. Tungate,[2] and J. Äystö[3]

[1]*Schuster Building, The University of Manchester, Brunswick Street, Manchester, M13 9PL, United Kingdom*
[2]*School of Physics and Astronomy, The University of Birmingham, Birmingham, B15 2TT, United Kingdom*
[3]*Department of Physics, University of Jyväskylä, PB 35 (YFL) FIN-40014 Jyväskylä, Finland*
[4]*Institut für Physik, Johannes Gutenberg Universität Mainz, Staudinger Weg 7, D-55128 Mainz, Germany*

(Received 18 January 2009; published 5 June 2009)

A new method of optical pumping in an ion beam cooler buncher has been developed to selectively enhance ionic metastable state populations. The technique permits the study of elements previously inaccessible to laser spectroscopy and has been applied here to the study of Nb. Model independent mean-square charge radii and nuclear moments have been studied for $^{90,90\,m,91,91\,m,92,93,99,101,103}$Nb to cover the region of the $N = 50$ shell closure and $N \approx 60$ sudden onset of deformation. The increase in mean-square charge radius is observed to be less than that for Y, with a substantial degree of β softness observed before and after $N = 60$.

DOI: 10.1103/PhysRevLett.102.222501 PACS numbers: 21.10.Ft, 21.10.Ky, 27.60.+j

Collinear laser spectroscopy has for many years been used to provide the (sole) model-independent probe of charge distributions of radioactive nuclei [1]. Efficient optical measurements are typically limited to transitions from atomic (or ionic) ground states or naturally populated low-lying metastable states. However, elements around $Z = 40$ such as Y, Nb, and Mo present a variety of challenges to such spectroscopic approaches. In this Letter, we report a new, general technique of wide applicability, in which radio ions are deliberately prepared in metastable states by a rapid and efficient method of optical pumping. The technique is exploited here in the spectroscopic study of the $A = 100$ region.

The well-known onset of deformation in the neutron-rich $A \approx 100$ region has been of long standing interest and the subject of recent mass [2,3], γ-ray spectroscopic [4,5], and optical measurements [6,7]. Collinear laser spectroscopy of Y isotopes was recently performed [6] in order to extract quadrupole moments in the region for comparison with charge-radii systematics. It was seen that with increasing neutron number from the $N = 50$ shell closure, the nuclear deformation becomes increasingly oblate and increasingly soft. At $N = 60$, the transition to a strongly deformed rigid prolate shape occurs, but prior to this, although the nuclear deformation is increasing with N, a proportionate increase in softness is also observed. Mass measurements [2,3] have indicated that the shape change, which is most pronounced for $_{39}$Y, weakens with increasing Z, becoming almost undetectable in the $_{42}$Mo chain. Further detailed model-independent optical analysis of the mean-square charge radii, nuclear moments and values of spin has so far, however, been impossible in the region because of experimental atomic physics constraints.

Production of radioactive beams in this region, which are of a refractory nature, is presently limited to relatively small yields, and efficient spectroscopy is therefore required. Such elements are produced for optical study at the JYFL IGISOL facility, University of Jyväskylä, Finland [8]. Following mass selection at this on-line separator, the emittance of the ion beam is reduced in an ion beam cooler [7], which is a gas-filled rf quadrupole, held at a potential just below the $\sim$30 kV of the ion source. If desired, a trapping potential can accumulate the ions at the end of the device for 10–500 ms before releasing them in bunches of 15 μs temporal length, for reacceleration to 30 keV. The cw light is provided by a high-resolution I_2-stabilized frequency-doubled dye laser. A tuning potential is applied to the collinear laser-ion interaction region to Doppler shift the light onto resonance. The nonresonant photon background is suppressed by $\sim 10^4$ by applying a gate to the photon signal which defines the interaction of the ion bunch with the laser beam [7].

For atomic systems around $Z = 40$, great difficulties are encountered in the spectroscopy of ground state ions or charge exchanged neutral fast beams. In the cases of Y and Nb, $J = 0$ ionic ground states limit the spectroscopy to $J = 0 \rightarrow J = 1$ transitions. An efficient 363.4 nm transition of this type was used for Y [6], permitting the extraction of the magnetic dipole moment, electric quadrupole moment and change in mean-square charge radius. However, the values determined for these quantities depended on the nuclear spin assignments which were unconfirmed for the $^{98\,m,100,102}$Y isotopes. Likewise, the Nb transitions are similarly restricted, posing a problem for key $N \geq 60$ isotopes. Values of nuclear spin may only be gained if a measurement of these isotopes is made using a transition from a metastable state of higher J. Moreover, the only Nb ground state transition accessible to the high-resolution cw laser, at 286.6 nm, suffers from a low oscillator strength and low population (which is spread through

the states of a low-lying multiplet). Ground state transitions of the adjacent Mo chain are all in the region $\lambda \leq 208.2$ nm and beyond the cw laser's capability. Charge exchange of the ions to neutral atoms would lead to populations in a region of high level density and also suffer from weak oscillator strengths.

In the approach reported here, the central axis of the ion beam cooler is illuminated with laser light. This axis defines the containment region of the slowly travelling ions, both inside the gas volume and in an 800 V transfer section. Efficient optical pumping is made possible due to the extended laser-ion interaction time in the trap. Broadband lasers may be used to pump this region where resonances are broadened by the trap motion and the linewidth of 20 GHz matches well the linewidth of the pulsed titanium-sapphire (Ti-Sa) lasers. Using high power pulsed Ti-Sa lasers readily permits the production of the 2nd, 3rd, and 4th harmonics, and therefore access to a greater range of wavelengths than the cw lasers used for spectroscopy. The excited state will then decay to populate metastable states, from which, high-resolution collinear spectroscopy is performed.

During efficiency tests, frequency quadrupled laser light was used to excite a 224.4 nm Y resonance. The ground state population, probed using collinear spectroscopy of a 311.3 nm line, is shown in Fig. 1 to be completely depopulated. The observation indicates that the entire ion ensemble was optically pumped, and that excitation takes place within the gas volume of the cooler, as the ions transit of the 800 V section was short in comparison to the duty cycle of the laser (12 kHz).

Figure 2 shows an excitation scheme for Nb. Although the 286.6 nm transition has only a weak oscillator strength, the longer exposure time ensures efficient pumping. With this optical pumping, the 290.9 nm transition was found to have the highest optical detection efficiency, which exceeded that of the Zr study [7]. In common with other cases explored, the magnitude of the resonance signal persisted on holding the ions in the cooler for hundreds of milliseconds before release. This is in marked contrast to unpumped ensembles, where the fluorescence intensity decreases rapidly ($\tau_{1/2} \approx 10$ ms) as the metastable state population relaxes inside the cooler.

Pumping transitions are selected according to their decay properties, with a metastable state *directly* populated via a strong branching ratio generally chosen for spectroscopy. The strong enhancement of the metastable state transition shown in Fig. 2 is unusual, given that the direct photon decay from the 34886 cm^{-1} level should only weakly enhance the 2357 cm^{-1} state. Such indirect enhancements have been explored in other systems, and pumping to populate states above 1 eV is typically observed to result in relaxation, and a redistribution of the population amongst lower-lying metastable levels via nonradiative transitions.

Neutron-deficient isotopes of Nb were produced using a 33 MeV ^{93}Nb(p, pxn)$^{90,90\,m,91,91\,m,92}$Nb reaction and used to calibrate the atomic factors. Isotopes of ^{99,101,103}Nb were produced at the IGISOL using proton-induced fission of ^{nat}U at 30 MeV. A thin foil of natural ^{93}Nb was inserted into the partitioned ion guide to provide stable ions as a spectroscopic reference. Reaction products were mass analyzed, cooled, and released in bunches, during which time the cooler axis was illuminated and the 286.6 nm transition saturated with 2 mW of light from a frequency-tripled Ti-Sa laser. A stabilized cw dye laser provided 1.2 mW of 290.9 nm light, which was focused and overlapped with the 30 keV ion beam. Frequency scans were taken by applying a tuning voltage to the region of interaction and a 15 μs gate was applied to the fluorescence signal. Sample spectra are shown in Fig. 3.

A χ^2 minimization technique was used to fit Voigt profiles to the data. The fitting yielded the centroid of the

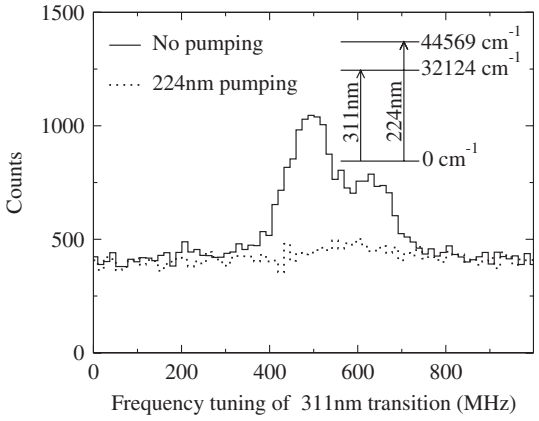

FIG. 1. Hyperfine resonances of a continuous Y^+ ion beam, observed using collinear spectroscopy of the 311.3 nm ground state line. A few mW of 224.4 nm light in the cooler buncher is seen to completely depopulate the ground state.

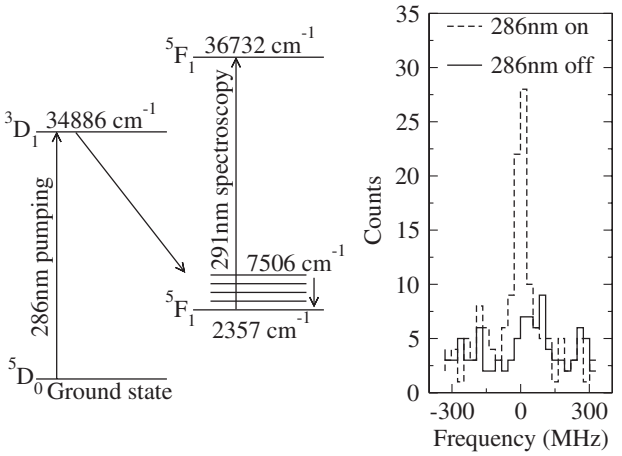

FIG. 2. Optical pumping scheme used for Nb. The effect of the 286.6 nm pumping light on the 290.9 nm fluorescence signal, the $F = 9 \rightarrow F = 9$ component of $^{90\,g}$Nb, is shown.

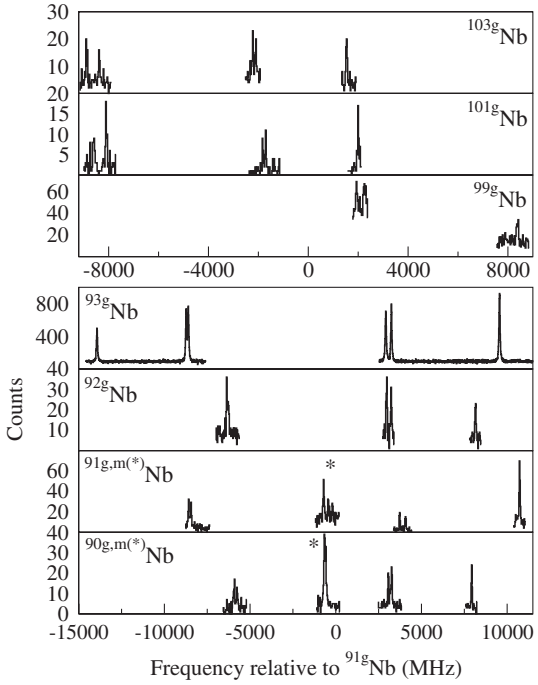

FIG. 3. Collinear fluorescence spectra of Nb, measured on the 290.9 nm 2357 $\mathrm{cm}^{-1} 5s^5F_1 \rightarrow 36732\ \mathrm{cm}^{-1} 5p^5F_1$ line. Metastable state structures are indicated by an asterisk.

transition, ν, and the A and B hfs coefficients for the upper electronic state [1], with the lower state values constrained to match the atomic ratios observed in the ^{93}Nb data. The difference in centroid frequency between isotopes A and A', $\delta\nu^{A,A'} = \nu^{A'} - \nu^{A}$ is the isotope shift and the experimentally determined values are presented in Table I. By treating the nuclear spin as a free parameter and comparing the minimum χ^2, it was possible to unambiguously assign values of nuclear spin to the ^{92,101,103}Nb isotopes. On varying I, shifts in the fitted centroids and changes in component intensity occur, which, although most exaggerated for low values of I, still result in a confidence of $>4\sigma$ for $I = 7$ in ^{92}Nb.

TABLE I. Nb isotope shift measurements and hfs coefficients of the upper level, measured on the 290.9 nm 2357 $\mathrm{cm}^{-1} d^3 5s^5 F_1 \rightarrow 36\,732\ \mathrm{cm}^{-1} d^3 5p^5 F_1$ line.

A	I	A_{5p} (MHz)	B_{5p} (MHz)	$\nu^A - \nu^{91\,g}$ (MHz)
90 g	8	+540.6(4)	−1(7)	−115(8)
90 m	4	−4(2)	+43(6)	−190(9)
91 g	9/2	+1265.5(4)	+42(5)	0
91 m	1/2	−177(4)	⋯	−96(6)
92 g	7	+640.7(5)	+57(4)	−225(5)
93 g	9/2	+1197.5(2)	+52.9(8)	−588(3)
99 g	9/2	+1159(6)	+69(22)	−1856(21)
101 g	5/2	+1114.2(8)	−174(3)	−3419(4)
103 g	5/2	+1095.7(1.4)	−179(9)	−3792(4)

The magnetic dipole moment, μ, and spectroscopic electric quadrupole moment, Q_s, were extracted from the hfs coefficients using the known moments of ^{93}Nb as a calibration [9–11]. The isotope shift is related to the change in mean-square charge radius via

$$\delta\nu_i^{A,A'} = M\frac{A' - A}{AA'} + F\delta\langle r^2\rangle^{A,A'}. \quad (1)$$

The field factor, F, and mass parameter, M, can be calibrated using a King plot [12] of isotope shift values together with $\delta\langle r^2\rangle$ values from other sources. As no experimental $\delta\langle r^2\rangle$ values in Nb are known, an approximate technique [13] was used to generate estimates of $F = -2.43\ \mathrm{GHz}\cdot\mathrm{fm}^{-2}$ and $M = +716\ \mathrm{GHz}\cdot\mathrm{amu}$ from the neutron deficient $\delta\langle r^2\rangle$ values of the neighboring Zr chain [14]. The linearity of such modified King plots reflects the regional similarity of the nuclear size systematics. Table II summarizes the nuclear data extracted in this work. An additional 10% uncertainty, representative of the regional $\delta\langle r^2\rangle$ uncertainties, is assigned to the charge-radii results.

In common with other isotope chains in the region, Nb is seen here to undergo an onset of deformation at $N \approx 60$. Similar to Y, the deformation changes at this point from weakly oblate in character (prior to the shape change) to a strongly prolate shape. Figure 4 shows the experimental charge radii, where a sharp increase of $\delta\langle r^2\rangle = +0.703\ \mathrm{fm}^2$ is seen between $N = 58$ and $N = 60$. The value is however notably less than the corresponding value of $\delta\langle r^2\rangle = +0.928\ \mathrm{fm}^2$ observed in Y [6].

The static deformation parameter, $\langle\beta_2\rangle$, can be derived from the measured quadrupole moments assuming an axially symmetric shape and using

$$Q_0 \approx \frac{5Z\langle r^2\rangle_{\mathrm{sph}}}{\sqrt{5\pi}}\langle\beta_2\rangle(1 + 0.36\langle\beta_2\rangle), \quad (2)$$

$$Q_0 = Q_s\frac{(I+1)(2I+3)}{I(2I-1)}. \quad (3)$$

Following the shape change, a *much* smaller level of static deformation is seen in Nb, $\langle\beta_2\rangle(^{101}\mathrm{Nb}) = 0.27$, than the Y

TABLE II. Nuclear moments and mean-square charge radii, $\delta\langle r^2\rangle^{91\,g,A}$.

A	I	μ (μ_N)	Q_s (b)	$\delta\langle r^2\rangle^{91\,g,A}$ (fm^2)
90 g	8	+4.952(4)	+0.01(4)	+0.011(1)
90 m	4	−0.018(9)	−0.26(4)	+0.042(2)
91 g	9/2	+6.521(2)	−0.25(3)	⋯
91 m	1/2	−0.101(2)	⋯	+0.040(3)
92 g	7	+5.136(4)	−0.35(3)	+0.127(3)
93 g	9/2	+6.1705(3)[a]	−0.32(2)[a]	+0.312(2)
99 g	9/2	+5.97(3)	−0.42(14)	+1.028(12)
101 g	5/2	+3.190(2)	+1.05(7)	+1.731(2)
103 g	5/2	+3.137(4)	+1.08(9)	+1.942(2)

[a]Stable ^{93}Nb is used as a calibration [9–11].

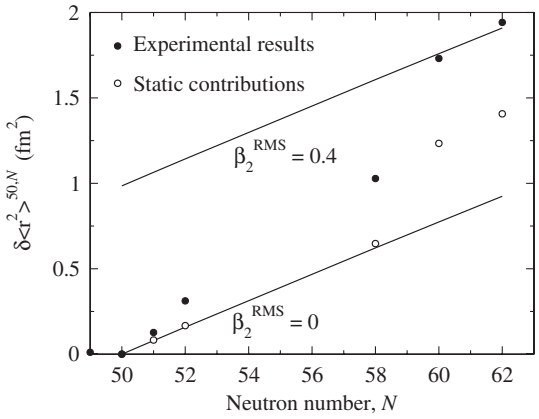

FIG. 4. Experimentally determined mean-square charge radii compared with contributions from static β_2 deformation alone. Droplet model isodeformation lines are included.

isotone, $\langle\beta_2\rangle(^{99}\mathrm{Y}) = 0.41$. Figure 4 includes estimates of the charge radii from the extracted $\langle\beta_2\rangle$ values, using

$$\delta\langle r^2\rangle = \delta\langle r^2\rangle_{\mathrm{sph}} + \langle r^2\rangle_{\mathrm{sph}} \frac{5}{4\pi} \delta\langle\beta_2^2\rangle, \tag{4}$$

where $\langle r^2\rangle_{\mathrm{sph}}$ is the mean-square charge radius of a spherical distribution with the same volume [15], and $\langle\beta_2^2\rangle$ is the mean-square quadrupole deformation. The influence of the contribution of the static deformation alone is studied by substituting the square of the static deformation parameter, $\langle\beta_2\rangle^2$, for the mean-square deformation, $\langle\beta_2^2\rangle$. The discrepancy between the static estimates and the experimental values of deformation can then be regarded as a measure of the β softness of the deformation.

Isotopes of Y show an increasing softness with N before adopting strong rigid prolate shapes following the onset of deformation [6]. This is compatible with calculated potential energy surfaces as a function of β_2 [16]. A flattening of the well bottom with increasing N followed by the formation of two distinct minima (one prolate and one oblate) is consistent with the observed quadrupole deformation. Triaxiality is not believed to significantly affect $\delta\langle r^2\rangle$, as Y (and Nb) isotopes are well described by axially symmetric shapes in this region [17].

By contrast however, isotopes of Nb show a markedly different behavior. Although the onset of deformation persists, and marks the change from weakly oblate to strongly prolate shapes, isotopes both before *and after* the shape change show a significant degree of β softness. The magnitude of the change in $\delta\langle r^2\rangle^{N=58,60}$ is slightly smaller in the case of Nb, and the difference in the static contribution to the $N = 60$ quadrupole deformation is more pronounced, indicating both a weakening and a softening of the deformation from Y to Nb. The behavior is very similar to that of the Rb chain [18]. The magnitude of the sudden onset of deformation at $N = 60$ thus appears to peak at $Z = 39$ (Y) and soften symmetrically about this point.

In-cooler optical pumping has been shown here to be an efficient, necessary, and widely applicable technique. A range of other pumping-assisted experiments are already underway at JYFL. The nature of the shape change (if present) in the Mo chain is under investigation using spectroscopy from the $4d^4 5s^6 D$ metastable levels. These are enhanced using 208.2 nm light from a frequency quadrupled pulsed Ti-Sa laser. Assignments of nuclear spin values in Y are in progress using 363.4 nm pumping to permit efficient spectroscopy of the 321.8 nm line from a 1045 cm^{-1} level. An alternative scheme has also been developed on the alkali-like Y^{2+} ion. In this case, measuring the 294.6 nm $s \rightarrow p$ transition from the 7467 cm^{-1} level greatly eases the process of theoretically calculating the field and mass shift factors of Eq. (1), and provides enhanced sensitivity to $\delta\langle r^2\rangle$ values. Elsewhere in the nuclear chart, optical spectroscopy of Ta isotopes is being studied on the 301.3 nm transition from the 5331 cm^{-1} level, enhanced via the excitation of the 225.0 nm ground state transition. Previous attempts to study Ta were hampered by the only efficient ground state transition possessing a large hfs anomaly and a large second-order mixing in the upper state [19].

This work has been supported by the UK STFC, the EU 6th Framework programme "Integrating Infrastructure Initiative-Transnational Access," Contract No. 506065 (EURONS) and by the Academy of Finland Centre of Excellence Programme 2006–2011 (Nuclear and Accelerator Based Physics Programme at JYFL).

*bradley.cheal@manchester.ac.uk

[1] E. W. Otten, in *Treatise on Heavy-Ion Science*, edited by D. A. Bromley (Plenum Press, New York, 1989), Vol. 8, p. 517.
[2] U. Hager *et al.*, Nucl. Phys. A **793**, 20 (2007).
[3] U. Hager *et al.*, Phys. Rev. Lett. **96**, 042504 (2006).
[4] C. Y. Wu *et al.*, Phys. Rev. C **70**, 064312 (2004).
[5] W. Urban *et al.*, Nucl. Phys. A **689**, 605 (2001).
[6] B. Cheal *et al.*, Phys. Lett. B **645**, 133 (2007).
[7] P. Campbell *et al.*, Phys. Rev. Lett. **89**, 082501 (2002).
[8] J. Äystö, Nucl. Phys. A **693**, 477 (2001).
[9] R. Sheriff and D. Williams, Phys. Rev. **82**, 651 (1951).
[10] H. Povel, Nucl. Phys. A **217**, 573 (1973).
[11] P. Pyykkö, Mol. Phys. **99**, 1617 (2001).
[12] W. King, *Isotope Shifts in Atomic Spectra* (Plenum, New York, 1984).
[13] W. Fischer *et al.*, Z. Phys. **270**, 113 (1974).
[14] H. L. Thayer *et al.*, J. Phys. G **29**, 2247 (2003).
[15] D. Berdichevsky and F. Tondeur, Z. Phys. A **322**, 141 (1985).
[16] J. Skalski *et al.*, Nucl. Phys. A **617**, 282 (1997).
[17] Y. X. Luo *et al.*, J. Phys. G **31**, 1303 (2005).
[18] C. Thibault *et al.*, Phys. Rev. C **23**, 2720 (1981).
[19] M. L. Bissell *et al.*, Phys. Rev. C **74**, 047301 (2006).